

Short Communication

Advanced Microscopy Techniques Used for Comparison of UVA- and γ -Irradiation-Induced DNA Damage in the Cell Nucleus and Nucleolus

(UVA / γ -irradiation / DNA damage response / nucleolus / living cell studies)

L. STIXOVÁ¹, T. HRUŠKOVÁ¹, P. SEHNALOVÁ¹, S. LEGARTOVÁ¹, S. SVIDENSKÁ², S. KOZUBEK¹, E. BÁRTOVÁ¹

¹Institute of Biophysics, Academy of Sciences of the Czech Republic, v. v. i., Brno, Czech Republic

²Institute of Cellular Biology and Pathology, First Faculty of Medicine, Charles University in Prague, Czech Republic

Abstract. Every day, genomes are affected by genotoxic factors that create multiple DNA lesions. Several DNA repair systems have evolved to counteract the deleterious effects of DNA damage. These systems include a set of DNA repair mechanisms, damage tolerance processes, and activation of cell-cycle checkpoints. This study describes selected confocal microscopy techniques that investigate DNA damage-related nuclear events after UVA- and γ -irradiation and compare the DNA damage response (DDR) induced by the two experimental approaches. In both cases, we observed induction of the nucleotide excision repair (NER) pathway and formation of lo-

calized double-strand breaks (DSBs). This was confirmed by analysis of cyclobutane pyrimidine dimers (CPDs) in the DNA lesions and by increased levels of γ H2AX and 53BP1 proteins in the irradiated genome. DNA damage by UVA-lasers was potentiated by either BrdU or Hoechst 33342 pre-sensitization and compared to non-photosensitized cells. DSBs were also induced without BrdU or Hoechst 33342 pre-treatment. Interestingly, no cyclobutane pyrimidine dimers (CPDs) were detected after 405 nm UVA laser micro-irradiation in non-photosensitized cells. The effects of UVA and γ -irradiation were also studied by silver staining of nucleolar organizer regions (AgNORs). This experimental approach revealed changes in the morphology of nucleoli after genome injury. Additionally, to precisely characterize DDR in locally induced DNA lesions, we analysed the kinetics of the 53BP1 protein involved in DDR by fluorescence recovery after photobleaching (FRAP).

Received June 27, 2014. Accepted July 21, 2014.

This work was supported by the *Education for Competitiveness Operational Programme* (ECOP) CZ.1.07/2.3.00/30.0030, and by the Grant Agency of the Czech Republic, project P302/12/G157.

Corresponding author: Lenka Stixová, Institute of Biophysics, Academy of Sciences of the Czech Republic, v. v. i., Královopolská 135, 612 65, Brno, Czech Republic. Phone: (+420) 541 517 141; Fax: (+420) 541240498; e-mail: lenka@ibp.cz

Abbreviations: AgNORs – silver-stained nucleolar organizer regions, ATM – ataxia telangiectasia mutated, ATR – ATM and Rad3-related, BER – base-excision repair, BrdU – bromodeoxyuridine, CPDs – cyclobutane pyrimidine dimers, DDR – DNA damage response, DMEM – Dulbecco's modified Eagle's medium, DNA-PK – DNA-dependent protein kinase, DSBs – double-strand breaks, FI – fluorescence intensity, FRAP – fluorescence recovery after photobleaching, GFP – green fluorescence protein, HR – homologous recombination, iMEFs – immortalized mouse embryonic fibroblasts, IR – ionizing radiation, IRIF – ionizing radiation-induced foci, NER – nucleotide excision repair, NHEJ – non-homologous end joining, NOR – nucleolar organizer region, PBS – phosphate-buffered saline, PCR – polymerase chain reaction, rDNA – ribosomal DNA, RNA Pol II – RNA polymerase II, ROI – region of interest, RPA – replication-related protein A, SDS – sodium dodecyl sulphate, UVA – ultraviolet A.

Introduction

Cells respond to genotoxic stress by activating DNA damage response (DDR) systems. During this process, DNA repair, cell cycle arrest, senescence, or apoptosis can be induced (Bartek and Lukas, 2007). Different types of DNA damage are recognized and processed by specific cellular response pathways that are able to repair the DNA damage, failing which the cells are eliminated by apoptosis. Multiple DNA repair pathways have evolved and activation of the appropriate DDR depends on specific types of DNA lesions (Hoeijmakers, 2001; Luijsterburg et al., 2009). Damage events that affect only one of the two DNA strands are removed by excision repair. Nucleotide excision repair (NER) removes UV-induced lesions consisting of cyclobutane pyrimidine dimers (CPDs), while oxidative lesions are mainly removed by base excision repair (BER). Damage events that affect both DNA strands are repaired by two funda-

mental cell cycle-related mechanisms, homologous recombination (HR) and non-homologous end joining (NHEJ) (summarized by Jackson and Bartek, 2009; Nagy and Soutoglou, 2009). Although many of these factors involved in the recognition and repair of DNA damage have been identified, how they participate in specific repair pathways *in vivo* is not fully understood.

Ionizing radiation (IR) produces DNA damage including single-, double-strand breaks and oxidative base damage. Inappropriately repaired DSBs can serve as a template for chromosomal translocations and mutations. For DSB repair studies, formation of ionizing radiation-induced foci (IRIF) is considered an indicator of DNA lesions and subsequent accumulation of key proteins can be evaluated. It is well known that IRIF can co-localize with DSB markers, including phosphorylated histone H2AX (γ H2AX) or 53BP1 (summarized by Kong et al., 2009).

The biological effects of UVA radiation on cells and skin is oxygen-dependent. Radiation-caused damage affects not only DNA or the entire chromatin, but also other cellular compounds including membranes, non-histone proteins and mitochondria. UVA is able to induce formation of CPDs, as summarized in the literature (Cadet et al., 2012). The yield of CPDs was found to be larger than 8-oxoGua, long thought to be the hallmark of UVA genotoxicity (Mouret et al., 2012). While bipyrimidine photoproducts are produced by direct excitation of the DNA bases, the formation of oxidatively generated lesions including 8-oxoGua obeys indirect photosensitized mechanisms. The photosensitizers can trigger several DNA oxidative pathways, specifically oxidation reactions mediated by singlet oxygen ${}^1\text{O}_2$, one-electron oxidation, and hydroxyl radical-mediated DNA damage (Miyamoto et al., 2003; Baumler et al., 2012; Cadet et al., 2012). After 8-oxoGua, the second most frequent UVA-induced DNA oxidatively generated lesions are strand breaks. Formation of strand breaks can be mediated by hydroxyl radical reactions and has a yield approximately three times lower than oxidized purines. Additional DNA oxidation products in UVA-irradiated cells are DNA-protein crosslinks (Cadet et al., 2012).

The distribution of UVA-induced DNA oxidation products may depend on many parameters including the UVA wavelength and radiation dose (Kong et al., 2009). It is well known that lasers of different wavelengths induce different types of DNA lesions and therefore induce different DNA repair pathways (summarized by Ferrando-May et al., 2013). Another important parameter that may affect the appearance of UVA-mediated DNA lesions is the cell type specificity. This was recently illustrated for melanocytes that are more susceptible to UVA-induced DNA damage than other cell types (summarized by Cadet et al., 2012).

After irradiation, a number of proteins are recruited to the region of damaged chromatin. The localization of these proteins to regions of DSBs can be visualized indirectly by fluorescence microscopy, using appropriate

antibodies. The immunofluorescence technique is effective for detecting proteins recruited to the DNA lesions. Therefore, a combination of immunofluorescence and micro-irradiation with focused laser beams can serve as a useful tool to induce multiple DSBs in a limited nuclear area where recruitment of new DNA repair-related proteins can be studied (Suzuki et al., 2011; Ferrando-May et al., 2013).

Sensitization of cells to UVA irradiation with bromodeoxyuridine (BrdU) was well described previously (Lukas et al., 2005). BrdU is a synthetic analogue of thymidine, which is incorporated into a newly synthesized DNA. After UV-light exposure, BrdU is photoactivated and creates single-strand breaks in the close proximity to the exposed region, which results in DSB formation. Similarly, Hoechst (Hoechst 33342 and 33258) can also sensitize DNA to UVA irradiation, which results in the formation of DSBs (Kruhlak et al., 2006; Dinant et al., 2007).

Induction of DNA damage by UVA-micro-irradiation has been intensively studied. However, a direct comparison of the results is problematic because all irradiated parameters (wavelength, UV dose, diameter of irradiated regions, etc.) are not always specified and detection methods may vary in between laboratories, resulting in different sensitivity (summarized by Ferrando-May et al., 2013). Here, we describe selected confocal microscopy techniques that investigate DNA damage-related nuclear events and DNA damage response (DDR) after UVA- and γ -irradiation. We compared induction of DNA lesions by 355-nm and 405-nm UVA lasers with and without BrdU or Hoechst 33342 pre-sensitization. The kinetic properties of the 53BP1 protein involved in DDR, measured by the FRAP technique, are also discussed.

Material and Methods

Cell cultivation, transfection and treatment

Mouse embryonic fibroblasts (MEFs; gift from Prof. Thomas Jenuwein at Max-Planck Institute of Immunobiology, Freiburg, Germany) were cultivated in Dulbecco's modified Eagle's medium (DMEM, Sigma-Aldrich, Prague, Czech Republic) with 10% foetal bovine serum and appropriate antibiotics. Cells were cultivated at 37 °C in a humidified atmosphere containing 5% CO_2 .

Transfections were performed using the reagent METAFECTENE™PRO (#T040-2.0, Biontex Laboratories GmbH, Planegg, Germany). Five μg of mCherry-BP1-2 pLPC-Puro plasmid DNA (fragment of p53-Binding Protein 1) (Addgene, Cambridge, MA) was used for transfection of MEFs cells.

Cells were treated at 70% confluence with 0.5 $\mu\text{g}/\text{ml}$ actinomycin D for 2 h (#A9415, Sigma-Aldrich, Prague, Czech Republic).

Induction of DNA lesions and confocal microscopy

For local micro-irradiation by UVA lasers (wavelengths 355 nm and 405 nm), the cells were seeded on μ -Dish 35mm Grid-500 (#81166, Ibidi, Planegg, Germany). The cells at 70% confluence were sensitized with 10 μ M 5-bromo-2'-deoxy-uridine (BrdU) for 16–18 h before local irradiation (Bartova et al., 2011; Sustackova et al., 2012). Hoechst 33342 was added to the medium (final concentration 0.5 μ g/ml) 5 min before local irradiation. DNA repair events were also examined without BrdU and Hoechst 33342 sensitization. For these experiments, we used confocal microscope Leica TSC SP-5 X (Leica Microsystems, Wetzlar, Germany), equipped with white light laser (WLL, 470–670 nm in 1 nm increments); argon laser (488 nm) and UV lasers (355 nm and 405 nm). We used magnification 64 \times /N.A. = 1.4. The cells were placed in a cultivation hood (EMBL Heidelberg, Germany) and heated to 37 °C. In addition, we used a specific “Air Stream” incubator to get 5% CO₂ for optimal cell cultivation. Defined regions of interest (ROIs) were irradiated with 100% laser output for 3 s. Laser intensity was not reduced using the acousto-optic tunable filter. Irradiation by UVA lasers 355 and 405 nm was performed at the following settings: 512 \times 512 pixels, 400 Hz, bidirectional mode, 96 lines, zoom 8–12. For scanning we used the following settings: 1024 \times 1024 pixels, 400 Hz, bidirectional mode, four lines, zoom 8–12, observation time 2 h. UVA-irradiated cells were fixed immediately or 2 h after micro-irradiation; we did not observe any differences in the studied proteins depending on the time of fixation up to 2 h. In experiments involving γ -irradiation of the whole cell population, cells were irradiated by 5 Gy of γ -rays with Cobalt-60 (60-Co) and fixed 2 h after irradiation.

Specification of radiation sources available in our laboratory

UVA laser, 355 nm: (Coherent, Inc., Santa Clara, CA) Laser power: 80 mW; irradiated area: 25.8 \times 10⁻⁸ cm²; irradiation time: 3 s; resolution for image acquisition: 512 \times 512; line average: 96; pixel size: 60.06 \times 60.06 nm; image size: 30.74 \times 30.74 μ m; total number of irradiated pixels: 24.455; irradiation time per pixel: 122 \times 10⁻⁶ s; peak power per pixel (intensity of irradiation): 3 \times 10⁵ W/cm²; overall dose per pixel (dose of radiation in mJ): 1.5 mJ/cm².

UVA laser, 405 nm: (Diode laser) Laser power: 50 mW; irradiated area: 25.8 \times 10⁻⁸ cm²; irradiation time: 3 s; resolution for image acquisition: 512 \times 512; line average: 96; pixel size: 60.06 \times 60.06 nm; image size: 30.74 \times 30.74 μ m; total number of irradiated pixels: 24.776; irradiation time per pixel: 121 \times 10⁻⁶ s; peak power per pixel (intensity of irradiation): 1.9 \times 10⁵ W/cm²; overall dose per pixel (dose of radiation in mJ): 0.9 mJ/cm².

γ -rays: Source: cobalt-60 (Chisostat, Chirana, Prague, Czech Republic). Cells were cultivated on 22.1 cm² cell cultivation plates at a density of 6.5 \times 10⁴ cells/cm² and

irradiated by 5 Gy of γ -rays (total dose). The irradiation time was 2–3 min and the distance of the radiation source from the samples was 110 cm.

Immunostaining of interphase nuclei

Immunohistochemical staining was performed according to Bartova et al. (2005). After cell fixation with 4% formaldehyde, the interphase nuclei were permeabilized with 0.1% Triton X-100 for 8 min, 0.1% saponin (Sigma-Aldrich, Hamburg, Germany) for 12 min, and then washed twice in PBS for 15 min. Incubation followed for 1 h at room temperature in 1% bovine serum albumin (BSA) dissolved in PBS. The slides were washed in PBS and incubated with rabbit polyclonal antibodies against γ H2AX (phospho S139; #ab2893, Abcam, Cambridge, UK) and anti-53BP1 (#ab21083, Abcam). Each antibody was diluted 1 : 100 in 1% BSA dissolved in PBS, followed by overnight incubation at 4 °C. The cells were washed twice in PBS for 5 min and incubated for 1 h with secondary antibody: Alexa Fluor® 594 Donkey Anti-Rabbit IgG (H+L) antibody (#A-21207, Molecular Probes, Eugene, OR). Secondary antibodies were diluted 1 : 200 in 1% BSA dissolved in PBS. Immuno-stained specimens were washed three times in PBS for 5 min and DAPI staining was used as a counter-stain.

For CPD staining, the cells were fixed in 4% formaldehyde for 10 min at room temperature, permeabilized sequentially in 0.5% Triton X-100 for 5 min on ice. DNA was denatured using 2M HCl for 30 min at room temperature. After washing five times with PBS, slides were blocked with 20% bovine serum albumin dissolved in PBS for 30 min at 37 °C, then washed five times with PBS, and incubated with anti-CPD antibody (#NMDND001, Cosmo Bio Co., Ltd., Tokyo, Japan) for 30 min at 37 °C. The cells were washed twice in PBS for 5 min and incubated for 30 min at 37 °C with secondary Alexa Fluor® 594 Donkey Anti-Mouse IgG (H+L) (#A-21203, Molecular Probes) antibody.

AgNOR staining

The cells were fixed with 4% formaldehyde for 15 min and treated with Triton X-100 (8 min) and saponin (12 min). After dehydration in 70%, 80% and 96% ethanol (cooled at -20 °C; for 1 min each), the nuclei were stained for 30 min in the dark using the following mixtures: Mixture A (2% gelatin dissolved in double distilled water [ddH₂O] and 1% formic acid). Mixture B (50% AgNO₃ dissolved in ddH₂O). The ratio of A and B was 1 : 2. The samples were then dehydrated in 96%, 80%, and 70% ethanol at room temperature for 1 min. Vectashield was used as a mounting medium.

Fluorescence recovery after photobleaching (FRAP)

FRAP experiments were performed using the Leica TSC SP-5 X confocal microscope (Leica Microsystems) with resolution 512 \times 512 pixels / 400 Hz and argon la-

ser (488 nm). Ten percent of laser intensity in bidirectional scanning mode was used for scanning and 100% laser power was used for FRAP. A rather high zoom (> 8) for bleaching was used in order to get sufficient power to bleach the area. Analysis of the acquired images was performed using LEICA LAS AF software (version 2.1.2.).

Data analysis

Images obtained with the confocal microscope were analysed by LEICA LAS AF software according to Sustackova et al. (2012). Fluorescence intensities (Fig. 4A) were determined in both the irradiated and non-irradiated region of the cell nucleus. Curves were normalized to 1 for the first data points before irradiation. The cells were micro-irradiated by 355 nm UVA laser at time 0 and monitored from 10 s up to 5 min after UVA-irradiation.

Results and Discussion

Here, we describe the possibilities for analysis of DNA damage and DDR using the confocal microscopy techniques. DNA damage was induced by UVA micro-

irradiation and γ -irradiation. Induction of the nucleotide excision repair (NER) pathway was revealed by immunofluorescence assay, showing an appearance of CPDs. DSB formation was confirmed by the presence of γ H2AX and 53BP1. After irradiation by 5 Gy of γ -rays or UVA-laser, we investigated whether CPDs appear in the DNA lesions (Fig. 1A). In addition, we studied DNA damage marker 53BP1 (Fig. 1B) and phosphorylated histone H2AX (γ H2AX) (Fig. 1C). We confirmed that γ -irradiation increased the levels and number of CPD foci, and 53BP1 and γ H2AX-positivity in DNA lesions was also increased. After both γ -irradiation and UVA-irradiation, we observed induction of the NER pathway, recognized according to CPDs. Moreover, DNA repair pathways leading to elimination of localized DSBs were revealed according to 53PB1 and γ H2AX-positive signals (Fig. 1A-C). The formation of DSBs was independent of the cell cycle phase, as was shown earlier (Suzuki et al., 2011), but DSBs were recognized by two basic, cell-cycle-dependent mechanisms: NHEJ (appearing in G1 phase) and HR (initiated in S/G2 phase) (summarized by Polo and Jackson, 2011).

A number of laboratories have studied the effects of several UVA lasers of different wavelengths on inducing

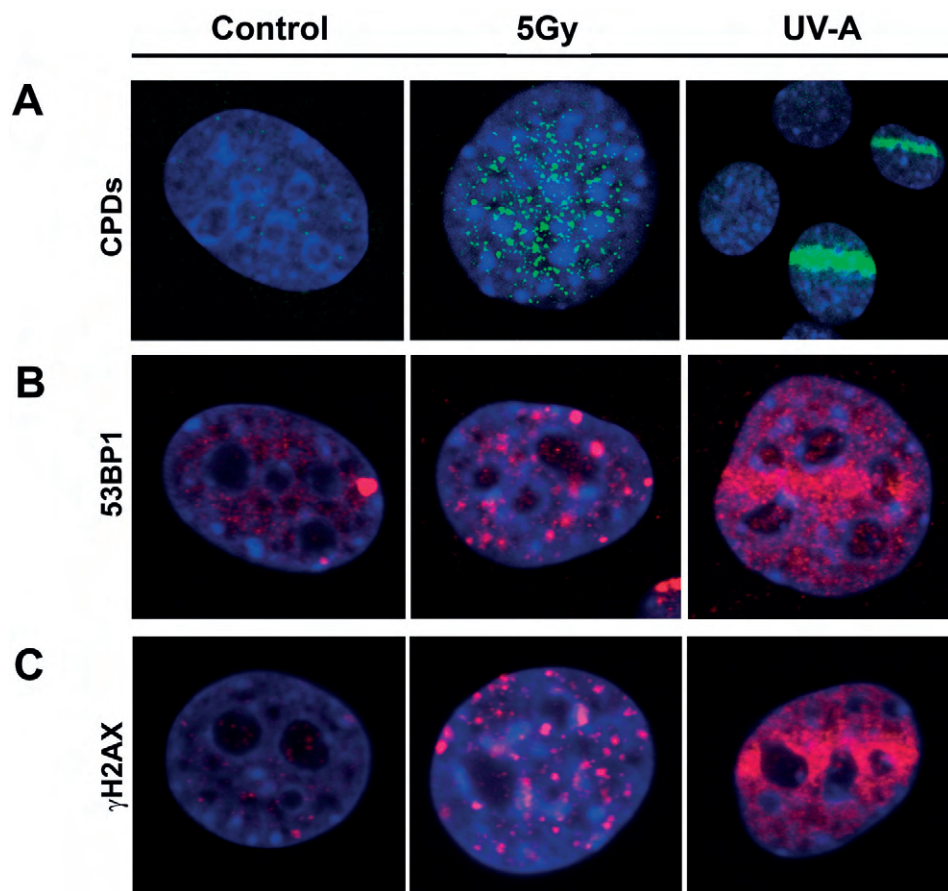


Fig. 1. An appearance of CPDs (A; green), 53BP1 (B; red) and γ H2AX (C; red) in γ -irradiated (5 Gy) or UVA-microirradiated cells. MEFs were exposed to 5 Gy of γ -rays or micro-irradiated by 355-nm UVA laser. Then the cells were fixed 2 h after γ -irradiation. For 355-nm UVA micro-irradiation, the cells were sensitized with 10 μ M BrdU for 16 h and after local micro-irradiation by UVA laser, cell nuclei were fixed with 4% formaldehyde and stained using appropriate antibodies that enable visualization of the presence of DNA damage markers.

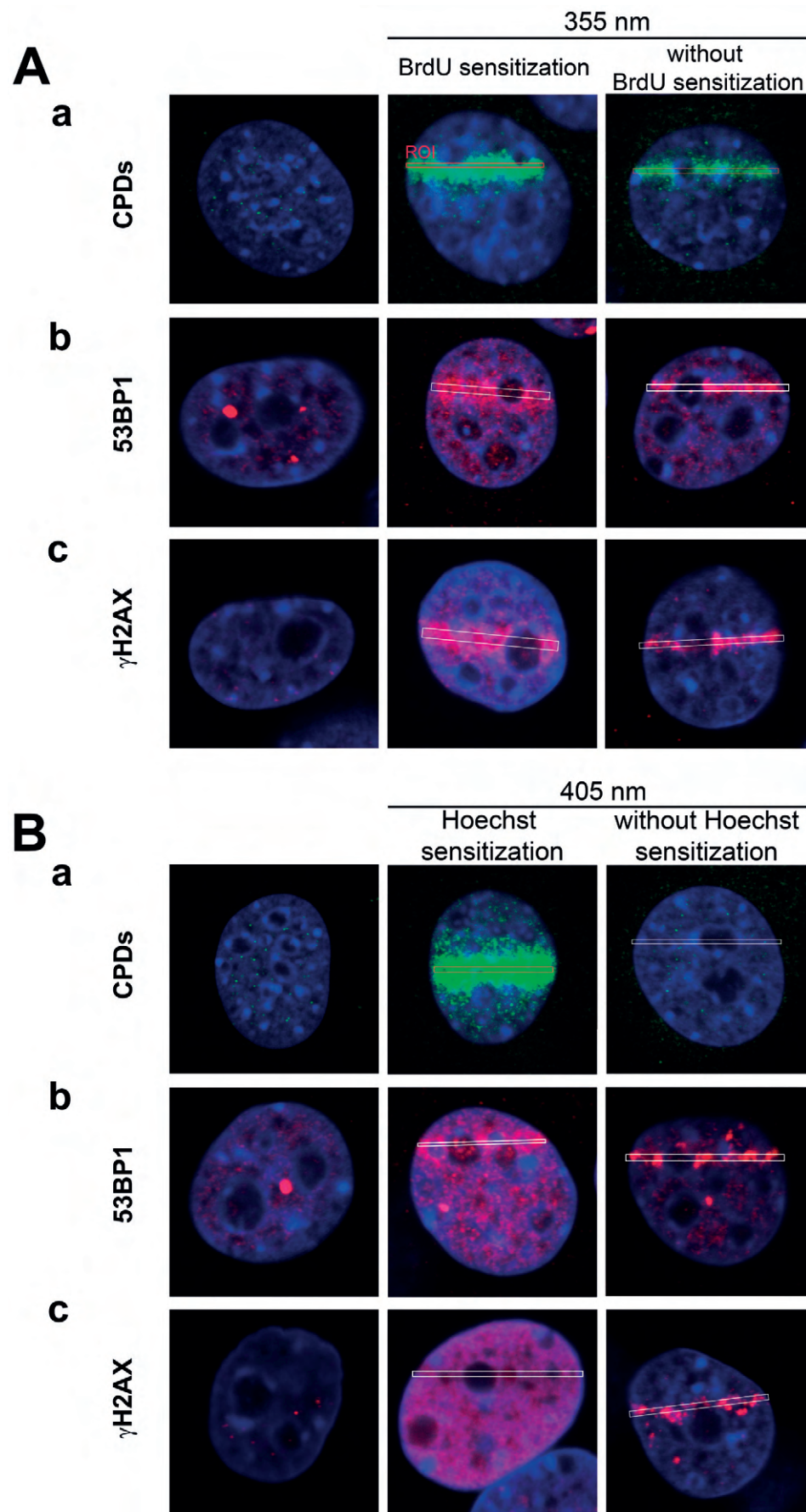


Fig. 2. Induction of different types of DNA lesions by 355-nm (A) and 405-nm (B) UVA lasers in BrdU- or Hoechst 33342-sensitized and non-sensitized cells. Immediately after UVA micro-irradiation, the cells were fixed and stained with antibodies specific for (a) CPDs, (b) 53BP1, and (c) γ H2AX.

DNA lesions (summarized by Ferrando-May et al., 2013). These methodological approaches were conducted in conjunction with pre-sensitization of DNA with various nucleotide analogues, including BrdU, 5'-iodo-2-deoxyuridine (IdU) or DNA-intercalating dyes (Hoechst 33342). These methods enabled study of the DNA damage response especially in living cells. GFP technologies also contribute to these experimental approaches by visualizing the protein recruitment to DNA lesions in time. Although contradictory results may be obtained using different laser systems (Kong et al., 2009), we compared the DNA lesions induced by 355-nm UVA laser with and without BrdU (Fig. 2A), and by the 405-nm UVA laser with and without Hoechst 33342 sensitization (Fig. 2B). After irradiation by 355-nm UVA laser, we observed the appearance of CPDs (Fig. 2Aa) or recruitment of 53BP1 (Fig. 2Ab) and γH2AX (Fig. 2Ac) at the irradiated area. For sensitization of cells before irradiation by 355-nm UVA laser, BrdU is routinely used (Lukas et al., 2003). This synthetic derivative of thymidine enabled us to increase formation of CPDs and DSBs and induce a more diffuse profile of the recruited proteins to DNA lesions, compared to cells without BrdU pre-sensitization, as shown in Fig. 2A (see dispersed fluorescence signals not only in ROIs). Similarly, Roukos et al. (2011) observed induction of DSBs after irradiation by 355-nm UVA laser.

In the case of 405-nm UVA laser, we first performed Hoechst 33342 sensitization according to Ayoub et al. (2008), but selected concentrations of Hoechst 33342 induced intensive DNA damage and apoptosis immedi-

ately after the treatment (data not shown). Then we used Hoechst 33342 sensitization according to Dinant et al. (2007) and analysed the effects of 405-nm UVA-micro-irradiation with and without this agent. We observed no recruitment of CPDs in non-sensitized MEF cells (Fig. 2Ba), but recruitment of 53BP1 (Fig. 2Bb) and γH2AX (Fig. 2Bc) was found. After Hoechst 33342 sensitization, we observed, similarly as Dinant et al. (2007), that DSBs and CPDs can be formed in the cells irradiated by 405-nm UVA laser, as shown in Fig. 2Ba-c. Our results indicate the involvement of different damage mechanisms dictated by the laser wavelength and laser intensity. The advantage of 405 nm UVA laser for the study on DDR is induction of DSBs without significant formation of CPDs. Thus, this experimental approach partially eliminates induction of various DNA repair pathways; only NHEJ or HR can be induced.

DNA damage typically affects the storage sites of the genetic material, such as the nucleolus (Foltankova et al., 2013). Therefore, we studied the changes in the morphology of nucleoli by silver staining of nucleolar organizer regions (AgNOR). This technique is routinely used for determination of cell proliferation in different types of tumours (summarized by Trere, 2000). This technique is based on the fact that acidic proteins, presented on active ribosomal genes of interphase nucleoli, are stained by silver (Ag) (Bhatt et al., 2013). Using AgNOR staining, it is possible to analyse the influence of γ-irradiation or UVA micro-irradiation on the morphology of nucleoli. In Figure 3, we show the morphology of AgNORs in non-irradiated cells (Fig. 3A) and

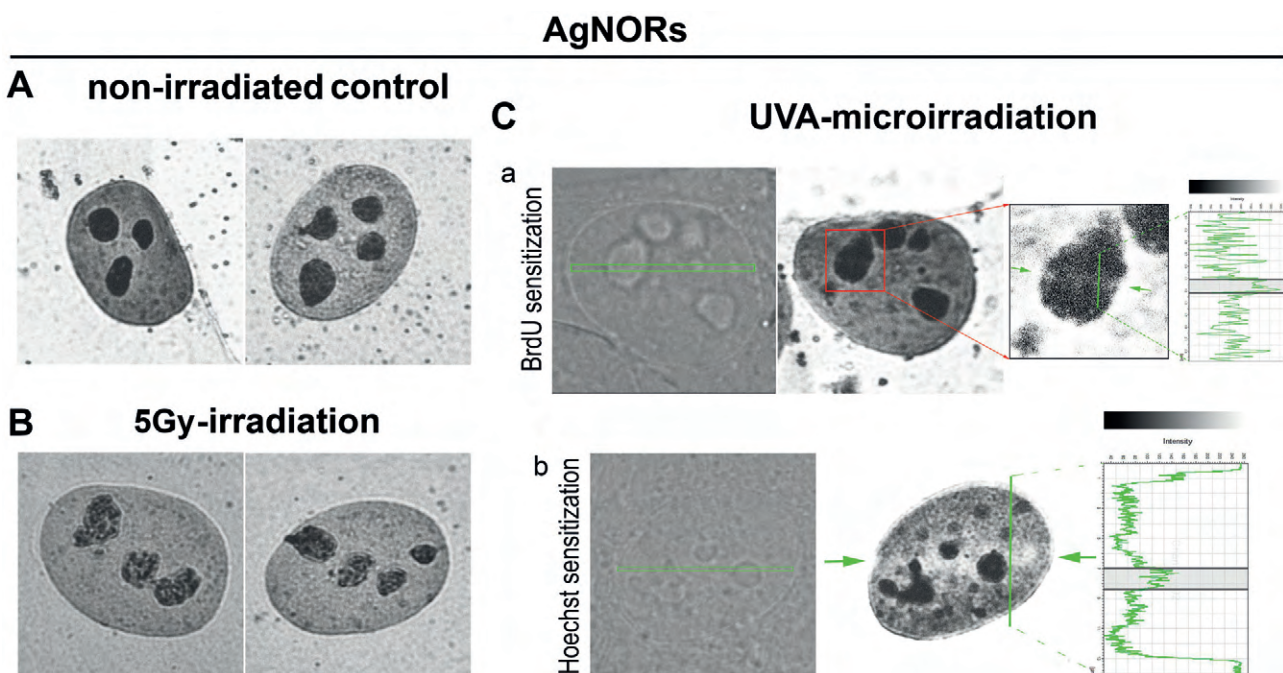


Fig. 3. Nuclear pattern of AgNORs in control non-irradiated cells and after γ-irradiation or UVA-micro-irradiation. Silver (Ag) staining of NORs was applied in (A) control non-irradiated MEFs, (B) cells exposed to 5 Gy of γ-rays, and (C) cells sensitized with (a) 10 μM BrdU and irradiated by 355-nm UVA laser or (b) cell sensitized with 0.5 μg/ml of Hoechst 33342 and irradiated by 405-nm UVA laser in the defined regions of interest (ROI; green). Quantification of cell nucleus and nucleolus densities was performed by LEICA LAS AF software (version 2.1.2.) as shown by enclosed graphs.

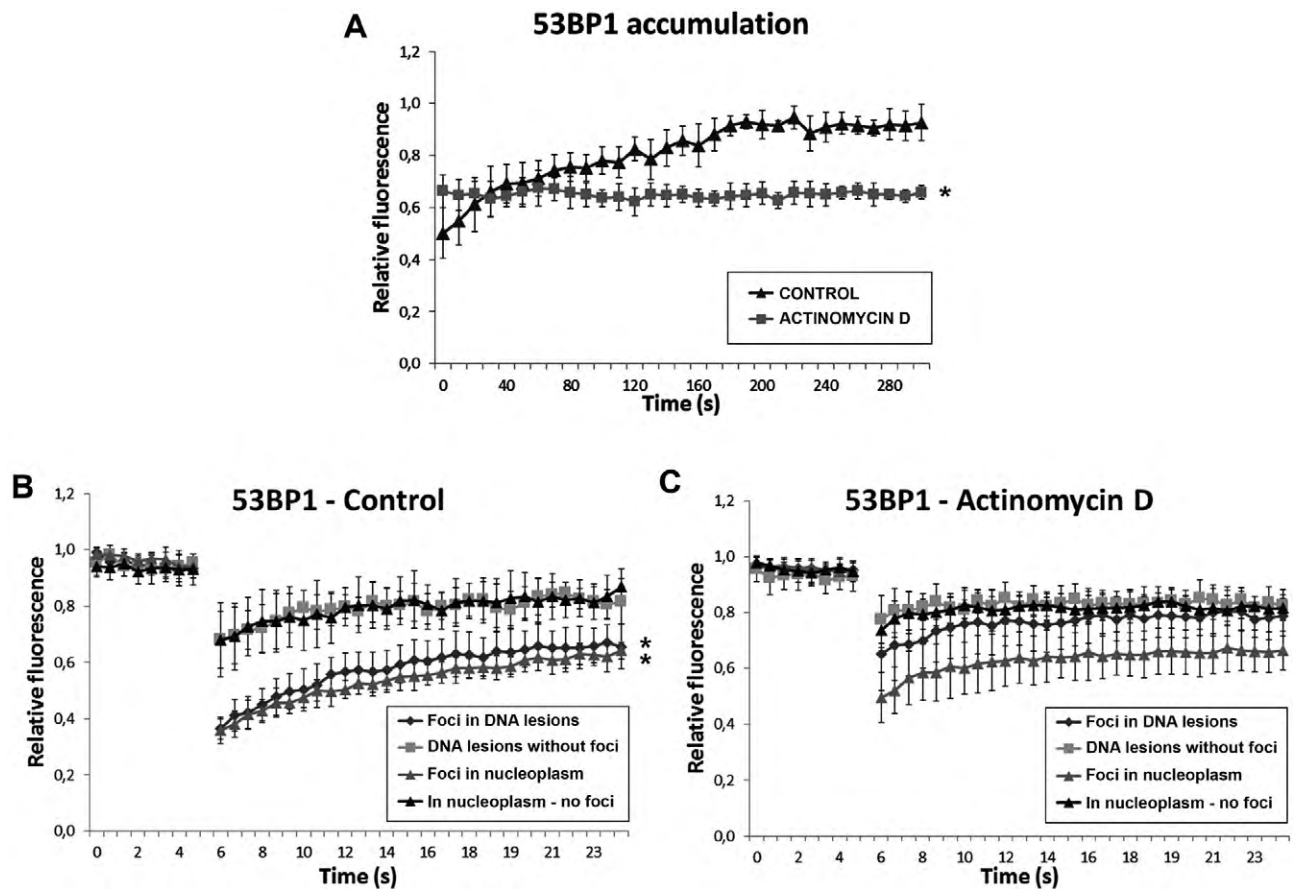


Fig. 4. Kinetics of mCherry-53BP1 after UVA micro-irradiation. (A) Time-lapse analysis of micro-irradiated MEF cells transiently transfected with plasmid DNA encoding 53BP1 sequences, tagged by mCherry. Control and cells treated with actinomycin D, 2 h before UVA-micro-irradiation, were sensitized with BrdU, micro-irradiated by 355-nm UVA laser in selected ROIs at time 0 and monitored from 10 s up to 5 min after UVA-irradiation. The intensity of mCherry-53BP1 fluorescence was normalized to 1. Statistically significant differences ($P \leq 0.05$) from the control are indicated with asterisks (*). Fluorescence recovery after photobleaching (FRAP) was measured for mCherry-53BP1 protein recruited to UVA-irradiated regions in (B) control, non-treated cells and (C) actinomycin D-stimulated MEFs. FRAP data were compared in irradiated nuclear area (grey squares), non-irradiated nuclear area (black triangles), and mCherry-53BP1 foci in irradiated area (dark diamonds) or mCherry-53BP1 foci in non-irradiated area (grey triangles). Statistically significant differences ($P \leq 0.05$) between the kinetics of mCherry-53BP1 localized in foci and surrounding nucleoplasm are indicated with asterisks (*).

AgNORs after γ -irradiation, which caused de-compaction of nucleoli (Fig. 3B). Similar effects were observed after UVA-microirradiation, which induced chromatin relaxation in both the nuclear and non-nucleolar regions, when damaged by UVA laser (Fig. 3C, arrows and quantification). This observation fits well with previously shown changes in chromatin compaction, considered as an important mark of DNA damage that accompanies DDR (Luijsterburg et al., 2012; Foltankova et al., 2013).

Proteomic analyses of the nucleolus (Moore et al., 2011) revealed that the nucleolus also contains several proteins involved in the cell cycle control and DNA damage response. These authors further showed that the proteome of the nucleolus is highly reorganized after exposure of cells to ultraviolet (UVC) irradiation, which induced alterations of specific protein complexes (Moore et al., 2011). Moreover, the DNA damage response in the nucleolus significantly differs between UV- and γ -irradiated genomes (Foltankova et al., 2013).

These results identified the nucleolus as a unique nuclear region, not only from the viewpoint of ribosome biogenesis, but also with regard to the DDR (Moore et al., 2011). Moreover, Andersen et al. (2005) demonstrated that the nucleolar proteome significantly changes over time during several cellular processes, including the stress response.

We also studied the effects of UVA irradiation on the dynamics of chromatin as well as the proteins involved in DDR by analysing the accumulation of the 53BP1 protein into the UVA-irradiated region (Fig. 4A). The kinetics of mCherry-53BP1 recruitment at DNA lesions is abrogated by inhibition of RNA polymerases using actinomycin D (Fig. 4A). The inhibitory effect of actinomycin D is similar to that observed for the protein GFP-Oct4, which is recruited to DNA lesions of mouse embryonic stem cells (Bartova et al., 2011). The kinetics of mCherry-tagged 53BP1 at UVA-induced DNA lesions was also studied by the FRAP technique. These

results do not show any significant differences in the kinetics of mCherry-53BP1 in irradiated and non-irradiated areas of control non-treated cells (Fig. 4B). Slower FRAP was observed for the mCherry-53BP1 protein accumulated in the foci when compared with the protein homogeneously dispersed in the nucleoplasm (Fig. 4B). Interestingly, actinomycin D did not influence the kinetics of mCherry-53BP1 localized away from the foci in both the irradiated and non-irradiated regions (Fig. 4C). However, increased recovery of fluorescence for mCherry-53BP1 protein was found when 53BP1 accumulated in the foci of the micro-irradiated region (Fig. 4C). This is in contrast to other studies of HP1 β , BMI1, TRF1 and PML proteins that do not show significant changes in fluorescence recovery after ActD when accumulated in nuclear foci (Stixova et al., 2011, 2012). It confirms that 53BP1 plays an important role during early response to DNA damage (Sehnalova et al., 2014; Fig. 4A).

We have shown that UVA- or γ -irradiation may induce multiple DNA repair mechanisms. Using advanced microscopy techniques, we investigated which DDR pathways became activated and precisely analysed the protein kinetics at DNA lesions of live cells. These approaches of advanced fluorescence microscopy could help to understand the DNA repair machinery in living cellular systems.

Acknowledgement

We thank Romaine Isaacs (Beltsville, MD) for English revision of our manuscript.

References

- Andersen, J. S., Lam, Y. W., Leung, A. K., Ong, S. E., Lyon, C. E., Lamond, A. I., Mann, M. (2005) Nucleolar proteome dynamics. *Nature* **433**, 77-83.
- Ayoub, N., Jeyasekharan, A. D., Bernal, J. A., Venkitaraman, A. R. (2008) HP1- β mobilization promotes chromatin changes that initiate the DNA damage response. *Nature* **453**, 682-686.
- Bartek, J., Lukas, J. (2007) DNA damage checkpoints: from initiation to recovery or adaptation. *Curr. Opin. Cell Biol.* **19**, 238-245.
- Bartova, E., Pachernik, J., Harnicarova, A., Kovarik, A., Kovarikova, M., Hofmanova, J., Skalnikova, M., Kozubek, M., Kozubek, S. (2005) Nuclear levels and patterns of histone H3 modification and HP1 proteins after inhibition of histone deacetylases. *J. Cell. Sci.* **118(Pt 21)**, 5035-5046.
- Bartova, E., Sustackova, G., Stixova, L., Kozubek, S., Legartova, S., Foltankova, V. (2011) Recruitment of Oct4 protein to UV-damaged chromatin in embryonic stem cells. *PLoS One* **6**, e27281.
- Baumler, W., Regensburger, J., Knak, A., Felgentrager, A., Maisch, T. (2012) UVA and endogenous photosensitizers – the detection of singlet oxygen by its luminescence. *Photochem. Photobiol. Sci.* **11**, 107-117.
- Bhatt, J., Shrimali, G., Patel, T., Sarvaiya, S., Modha, D., Gajjar, M. (2013) Silver stained nucleolar organizer region count (AgNOR count) – very useful tool in breast lesions. *Natl. J. Med. Res.* **3**, 280-282.
- Cadet, J., Mouret, S., Ravanat, J. L., Douki, T. (2012) Photoinduced damage to cellular DNA: direct and photo-sensitized reaction. *Photochem Photobiol.* **88**, 1048-1065.
- Dinant, C., de Jager, M., Essers, J., van Cappellen, W. A., Kanaar, R., Houtsmauller, A. B., Vermeulen, W. (2007) Activation of multiple DNA repair pathways by sub-nuclear damage induction methods. *J. Cell Sci.* **120(Pt 15)**, 2731-2740.
- Ferrando-May, E., Tomas, M., Blumhardt, P., Stockl, M., Fuchs, M., Leitenstorfer, A. (2013) Highlighting the DNA damage response with ultrashort laser pulses in the near infrared and kinetic modelling. *Front. Genet.* **4**, 135.
- Foltankova, V., Legartova, S., Kozubek, S., Hofer, M., Bartova, E. (2013) DNA-damage response in chromatin of ribosomal genes and the surrounding genome. *Gene* **522**, 156-167.
- Hoeijmakers, J. H. (2001) Genome maintenance mechanisms for preventing cancer. *Nature* **411**, 366-374.
- Jackson, S. P., Bartek, J. (2009) The DNA-damage response in human biology and disease. *Nature* **461**, 1071-1078.
- Kong, X., Mohanty, S. K., Stephens, J., Heale, J. T., Gomez-Godinez, V., Shi, L. Z., Kim, J. S., Yokomori, K., Berns, M. W. (2009) Comparative analysis of different laser systems to study cellular responses to DNA damage in mammalian cells. *Nucleic Acids Res.* **37**, e68.
- Kruhlak, M. J., Celeste, A., Dellaire, G., Fernandez-Capetillo, O., Muller, W. G., McNally, J. G., Bazett-Jones, D. P., Nussenzweig, A. (2006) Changes in chromatin structure and mobility in living cells at sites of DNA double-strand breaks. *J. Cell Biol.* **172**, 823-834.
- Luijsterburg, M. S., Dinant, C., Lans, H., Stap, J., Wiernasz, E., Lagerwerf, S., Warmerdam, D. O., Lindh, M., Brink, M. C., Dobrucki, J. W., Aten, J. A., Fousteri, M. I., Jansen, G., Dantuma, N. P., Vermeulen, W., Mullenders, L. H., Houtsmauller, A. B., Verschure, P. J., van Driel, R. (2009) Heterochromatin protein 1 is recruited to various types of DNA damage. *J. Cell Biol.* **185**, 577-586.
- Luijsterburg, M. S., Lindh, M., Acs, K., Vrouwe, M. G., Pines, A., van Attikum, H., Mullenders, L. H., Dantuma, N. P. (2012) DDB2 promotes chromatin decondensation at UV-induced DNA damage. *J. Cell Biol.* **197**, 267-281.
- Lukas, C., Bartek, J., Lukas, J. (2005) Imaging of protein movement induced by chromosomal breakage: tiny ‘local’ lesions pose great ‘global’ challenges. *Chromosoma* **114**, 146-154.
- Lukas, C., Falck, J., Bartkova, J., Bartek, J., Lukas, J. (2003) Distinct spatiotemporal dynamics of mammalian checkpoint regulators induced by DNA damage. *Nat. Cell Biol.* **5**, 255-260.
- Miyamoto, S., Martinez, G. R., Medeiros, M. H., Di Mascio, P. (2003) Singlet molecular oxygen generated from lipid hydroperoxides by the russell mechanism: studies using 18(O)-labeled linoleic acid hydroperoxide and monomol light emission measurements. *J. Am. Chem. Soc.* **125**, 6172-6179.
- Moore, H. M., Bai, B., Boisvert, F. M., Latonen, L., Rantanen, V., Simpson, J. C., Pepperkok, R., Lamond, A. I., Laiho, M. (2011) Quantitative proteomics and dynamic imaging of

- the nucleolus reveal distinct responses to UV and ionizing radiation. *Mol. Cell. Proteomics* **10**, M111 009241.
- Mouret, S., Forestier, A., Douki, T. (2012) The specificity of UVA-induced DNA damage in human melanocytes. *Photochem. Photobiol. Sci.* **11**, 155-162.
- Nagy, Z., Soutoglou, E. (2009) DNA repair: easy to visualize, difficult to elucidate. *Trends Cell Biol.* **19**, 617-629.
- Polo, S. E., Jackson, S. P. (2011) Dynamics of DNA damage response proteins at DNA breaks: a focus on protein modifications. *Genes Dev.* **25**, 409-433.
- Roukos, V., Kinkhabwala, A., Colombelli, J., Kotsantis, P., Taraviras, S., Nishitani, H., Stelzer, E., Bastiaens, P., Lygerou, Z. (2011) Dynamic recruitment of licensing factor Cdt1 to sites of DNA damage. *J. Cell Sci.* **124(Pt 3)**, 422-434.
- Sehnalova, P., Legartova, S., Cmarko, D., Kozubek, S., Bartova, E. (2014) Recruitment of HP1 β to UVA-induced DNA lesions is independent of radiation-induced changes in A-type lamins. *Biol. Cell.* **106**, 151-165.
- Stixova, L., Bartova, E., Matula, P., Danek, O., Legartova, S., Kozubek, S. (2011) Heterogeneity in the kinetics of nuclear proteins and trajectories of substructures associated with heterochromatin. *Epigenetics Chromatin* **4**, 5.
- Stixova, L., Matula, P., Kozubek, S., Gombitova, A., Cmarko, D., Raska, I., Bartova, E. (2012) Trajectories and nuclear arrangement of PML bodies are influenced by A-type lamin deficiency. *Biol. Cell* **104**, 418-432.
- Sustackova, G., Kozubek, S., Stixova, L., Legartova, S., Matula, P., Orlova, D., Bartova, E. (2012) Acetylation-dependent nuclear arrangement and recruitment of BMI1 protein to UV-damaged chromatin. *J. Cell Physiol.* **227**, 1838-1850.
- Suzuki, K., Yamauchi, M., Oka, Y., Suzuki, M., Yamashita, S. (2011) Creating localized DNA double-strand breaks with microirradiation. *Nat. Protoc.* **6**, 134-139.
- Trere, D. (2000) AgNOR staining and quantification. *Micron* **31**, 127-131.